Cyclones, tides, and the origin of a cross-equatorial dust storm on Mars

Huiqun Wang,[1] Mark I. Richardson,[1] R. John Wilson,[2] Andrew P. Ingersoll,[1]
Anthony D. Toigo,[3] and Richard W. Zurek[4]

Received 21 December 2002; revised 31 March 2003; accepted 7 April 2003; published 13 May 2003.

[1] We investigate the triggering mechanism of a cross-equatorial dust storm observed by Mars Global Surveyor in 1999. This storm, which had a significant impact on global mean temperatures, was seen in visible and infrared data to commence with the transport of linear dust fronts from the northern high latitudes into the southern tropics. However, other similar transport events observed in northern fall and winter did not lead to large dust storms. Based on off-line Lagrangian particle transport analysis using a high resolution Mars general circulation model, we propose a simple explanation for the diurnal, seasonal and interannual variability of this type of frontal activity, and of the resulting dust storms, that highlights the cooperative interaction between northern hemisphere fronts associated with low pressure cyclones and tidally-modified return branch of the Hadley circulation. *INDEX TERMS:* 5409 Planetology: Solid Surface Planets: Atmospheres—structure and dynamics; 6225 Planetology: Solar System Objects: Mars. **Citation:** Wang, H., M. I. Richardson, R. J. Wilson, A. P. Ingersoll, A. D. Toigo, and R. W. Zurek, Cyclones, tides, and the origin of a cross-equatorial dust storm on Mars, *Geophys. Res. Lett.*, *30*(9), 1488, doi:10.1029/2002GL016828, 2003.

1. Introduction

[2] Global and large regional dust storms represent an important component of the main martian climate cycles. They have been observed in the southern spring/summer "dust storm" season, and can increase the mid-level air temperatures by tens of Kelvin. The standard view of such storms assumes initiation and growth in the southern hemisphere, involving feedback between atmospheric circulation and radiative heating of dust [*Zurek et al.*, 1992]. Stochastic and surface dust redistribution processes have been invoked to explain the interannual variability of these storms [*Haberle*, 1986; *Pankine and Ingersoll*, 2002], yet a clear linkage between different processes and the triggering of storms is still missing. Daily global mapping by the Mars Global Surveyor (MGS) Mars Orbiter Camera (MOC) has yielded an unprecedented view of the martian atmosphere [*Cantor et al.*, 2001; *Wang and Ingersoll*, 2002]. These and other observations have shown that different types of large dust storms occur. While some apparently originate near topographic slopes in the southern hemisphere, others have more complex histories, involving low-pressure cyclones in the northern hemisphere [*Cantor et al.*, 2001].

[3] The largest dust storm in the first MGS mapping year (Ls = 220°–226°) was an event that produced a significant increase (5–10K) in midlevel atmospheric temperatures (Figure 1) [*Smith et al.*, 2001; *Liu et al.*, 2003]. This particular event originated in the northern hemisphere. Several bands of dust and were transported southward through Acidalia-Chryse across the equator, possibly augmented by additional dust lifting during transit (Figure 1) [*Cantor et al.*, 2001]. These successive transport events resulted in increased dust opacity in the region southeast of Valles Marineris. The dust was then rapidly spread in longitude to encircle the planet by the strong southern subtropical jet [*Liu et al.*, 2003]. The strong correlation between the arrival of dust in the upwelling branch of the Hadley cell and the generation of strong temperature increases observed by the MGS Thermal Emission Spectrometers (TES) (Figure 1c) [*Smith et al.*, 2001; *Liu et al.*, 2003] suggests that this event resulted from the cumulative effect of the southward moving storms. This is consistent with general circulation model (GCM) simulations, which suggest that accumulation of dust in the Hadley convergence zone will lead to atmospheric warming and intensification of the global circulation [*Haberle et al.*, 1982; *Wilson*, 1997]. MGS observed other southward moving dust fronts that did not generate significant impact on global air temperature. However, they were more isolated in time, and/or failed to penetrate as far south. Observationally, then, the repeated transport of dust into the Hadley convergence zone appears to be the key to the development of the largest dust storm of the first MGS mapping year. In this paper, we focus on the triggering mechanism, i.e. what differentiates northern hemisphere fronts that penetrate southward to low latitudes and generate storms of global impact from the common frontal systems that remain confined to mid latitudes?

[4] Figure 1 illustrates two southward moving dust storms that lead to the large dust storm described above. Fronts are indicated by linear belts of dust presumably lofted by strong near surface winds. Fronts stretch across Acidalia on the lee side of Tharsis as they propagate eastward at 20–28 m/sec. The fronts appear to be associated with low pressure cyclones [*James et al.*, 1999] that are associated with baroclinic waves [*Barnes et al.*, 1993]. The propagation speeds are consistent with a zonal wave 1 (a single wave cycle around a latitudinal circle) with a period of ~6 sols or a wave 3 with a period of ~2 sols. These periods agree with other observations and simulations [*Barnes et al.*, 1993; *Hinson and Wilson*, 2002; *Wilson et al.*, 2002]. While frontal dust storms are common in the northern high

[1]Division of Geological and Planetary Sciences, California Institute of Technology, Pasadena, California, USA.
[2]NOAA/Geophysical Fluid Dynamics Laboratory, Princeton, New Jersey, USA.
[3]Center for Radiophysics and Space Research, Cornell University, Ithaca, New York, USA.
[4]Jet Propulsion Laboratory, California Institute of Technology, Pasadena, California, USA.

0094-8276/03/2002GL016828

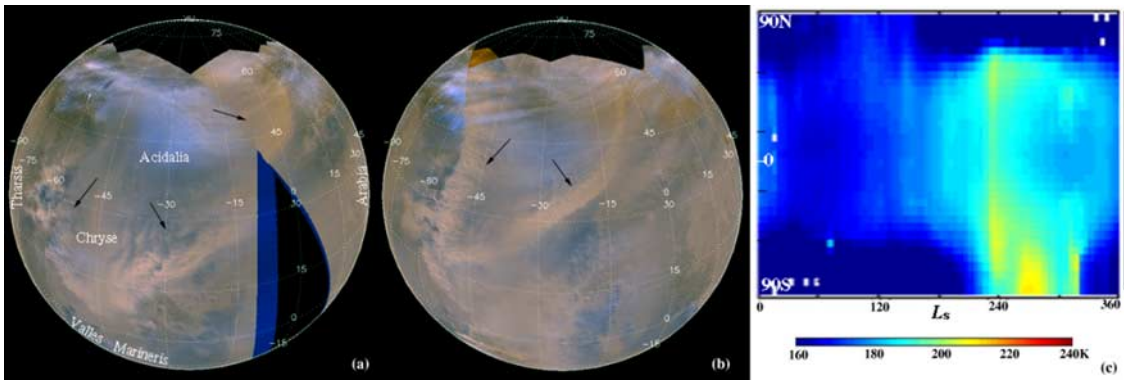

Figure 1. (ab) MGS MOC images of southward moving storms. They lead to the largest dust storm of MGS mapping year 1 (Ls 220°–226°). (c) Mid-level (~20 km) air temperatures observed by TES in MGS mapping year 1.

latitudes in southern spring and summer, only a small subset are observed to transport dust significant distances southwards.

[5] Southward moving dust fronts occurred multiple times during southern spring and summer in MGS mapping year 1 and 2 (from 1999 to 2001), but were limited to two seasonal periods: Ls = 210°–230° and Ls = 310°–350°. About a dozen individual events have been observed within each seasonal window. All of them have occurred in low-elevation channels in the northern hemisphere, most are associated with Acidalia-Chryse, and some with Arcadia-Amazonis and Utopia. In MGS mapping year 1, most events were concentrated in the Ls = 210°–230° period, with several after Ls = 310°. In MGS mapping year 2, following the 2001 global dust storm (Ls ~185°) [*Smith et al.*, 2002], all such events were observed in the Ls = 310°–350° period. The observations pose a number of questions: What causes frontal storms to move southward? Why do only some frontal storms move southward? Why are there two seasonal windows for such events? Why do they follow three primary low-elevation channels? Why do some southward moving dust fronts lead to dust storms of global impact? Why is there interannual variability in large dust storms generated by southward moving fronts?

2. Analysis With GCM

[6] This study uses a high resolution (2° × 2.4°) version of the Geophysical Fluid Dynamics Laboratory (GFDL) Mars GCM, which was run for a full martian year [*Wilson and Hamilton*, 1996; *Richardson and Wilson*, 2002]. In order to understand the southward moving dust fronts, we used an off-line Lagrangian particle transport model [*Eluszkiewicz et al.*, 1995] to analyze the transport capacity of the 92 simulated low pressure cyclones that passed through Acidalia during Ls = 200°–355°. For each storm, weightless passive particles were initialized from the surface to 2.5km in the box from −94.7°E to −63.7°E and from 49.5°N to 71°N, and were subsequently advected by the GCM wind field. The evolving particle distributions show that the simulated winds can concentrate particles into linear belts similar in shape, size, and propagation speed to the dust fronts observed by MOC (Figures 1 and 2), suggesting that southward moving dust fronts are associated with eastward traveling baroclinic storms.

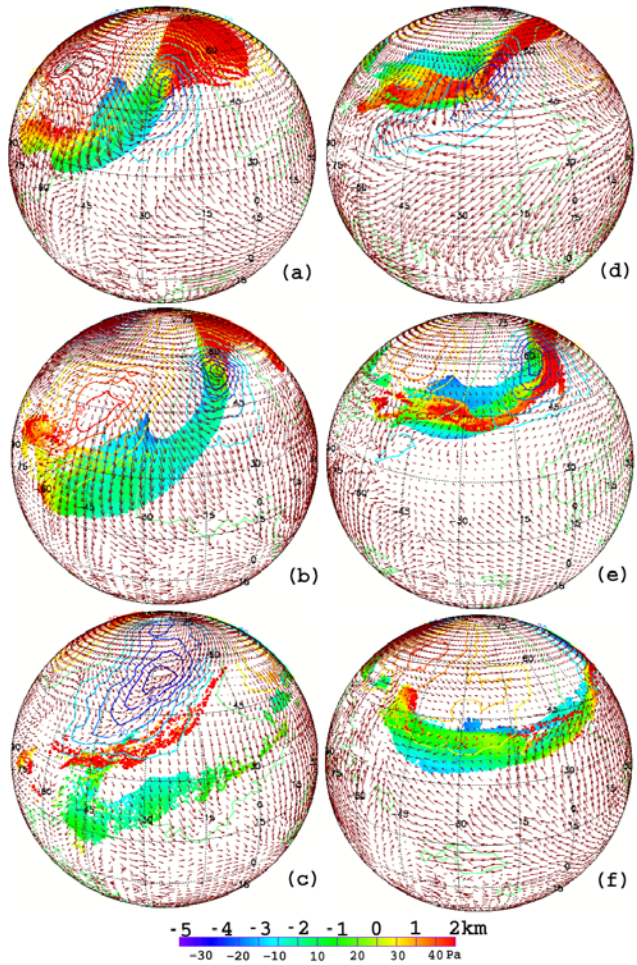

Figure 2. Lagrangian particle evolution for a front (a–c) with significant southward motion at Ls 342° and (d–f) without significant southward motion at Ls 354. The projection is that used in Figure 1. The altitudes of the particles are color-coded above the color bar. High particles are plotted above low ones. Simultaneous ~130 m model winds and surface pressure perturbation (contours, color-coding below the color bar) are shown. The particles are advected for 16 hr in (a, d), 48 hr in (c, f), 24 hr in (b) and 28 hr in (e). Low pressure centers pass 0°E in (b, e). The local time at −35°E is (b) 11:40 am and (e) 3:40 am.

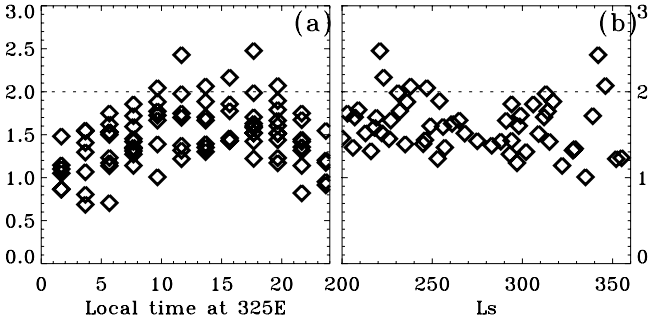

Figure 3. (a) Mean southward particle transport rate (°latitude/2 hours) as a function of local time at 325°E from Lagrangian analysis. The dashed line at 2°/2 hr corresponds to the rate necessary to transport particles to the southern hemisphere within ~2 sols. (b) The seasonal dependence of southward motion rates for storms that traversed Acidalia between 0900–1900 LT.

[7] In some experiments, a significant number of particles are advected into the low latitudes within 1 sol and into the southern hemisphere within a little over 2 sols (Figures 2a–2c). In other experiments, the particles did not extend to the low latitudes, and were eventually advected back to the northern high latitudes (Figures 2d–2f). The average rate of southward particle transport was derived by dividing the southward distance traveled by the time spent when the low pressure center passes 0°E. This rate depends upon a number of factors, but the most important ones were local solar time and Ls (Figure 3). Storms with significant southward motion only occurred when the low-pressure center passed 0°E during the local time interval from 9 am to 7 pm at −35°E in Acidalia. At these times, the tidal winds in Acidalia-Chryse are southward, and can interfere constructively with the frontal winds, generating strong southward transport. In other words, these storms passed through Acidalia through an opened "tidal gate", and the particles are advected into the southern hemisphere in ~2 tidal cycles. At other local times, tidal winds oppose frontal winds (Figures 2d–2f), corresponding to a closed "tidal gate" that prohibits effective southward frontal motion.

[8] The seasonality of the simulated southward transport event is shown in Figure 3b. The distinct decrease in such storms around solstice was found to be associated with a transition from a simulated zonal wave 2 or 3 away from the solstice, to a dominant wave 1 at solstice. Since simulated frontal winds associated with zonal wave 1 are usually weaker than those associated with wave 2 and 3, they do not interact strongly with the tidal winds. The longer periods [*Wilson et al.*, 2002] also result in fewer opportunities for fronts to interact with an "open gate". Wavelet analysis of the simulated mid-level wind field shows that before and after northern winter solstice, there is eddy activity with periods ranging from 2–7 sols extending from the northern midlatitude storm zone to the equator. The general interaction of the wave 1 fronts with the tides in multiple model years and the relationship between the mid-level eddy activity and the modeled southward particle motion will be investigated in the future. The southward extension of fronts is influenced by other factors such as the latitude of the low pressure center, and the strength and timing of the trailing high pressure. However, when the southward motion rate is plotted against these factors, we found no systematic trends. So, the "tidal gate" and "seasonal window" provide the most important conditions for southward transport of particles.

[9] Examination of the simulated surface stresses shows that storms with significant southward motion are associated with coherent broad regions of high surface wind stresses in Acidalia-Chryse (Figure 4d). This results from the constructive interference between the tidal and frontal winds. To investigate the potential for dust lifting, we performed off-line Lagrangian particle experiments with the particles injected whenever the simulated surface stress exceeds a threshold (0.0275 N/m^2, Figure 4). A curved front can still be identified within the first sol with similar southward motion rate. This particular event was associated with a wave 3 pattern. Many particles are picked up along the way by the front, consistent with the secondary storm centers in some southward moving dust fronts observed by MOC [*Cantor et al.*, 2001]. Similar experiments for fronts without significant southward motion show that particles associated with the baroclinic fronts tend to stay at northern high latitudes. Although there are occasional particle injections in Acidalia-Chryse, the injection areas are small and particles are separate from those in the baroclinic fronts. They appear as isolated small dust storms, instead of a part of a continuous southward moving front.

[10] Both the modeled and observed southward moving storms develop in three channels: Acidalia-Chryse, Arcadia, and Utopia Planitias. These regions correspond to the

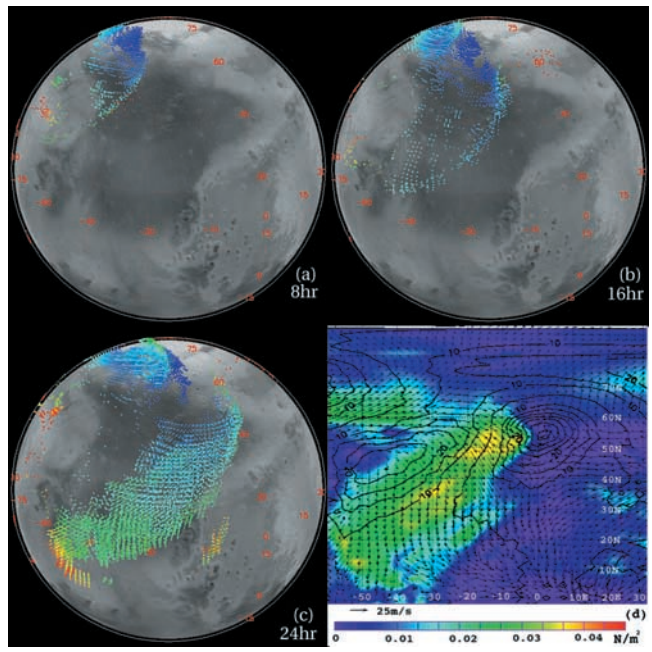

Figure 4. Particle distribution maps using interactive injection (Ls 342°) for (a) 8, (b) 16, (c) 24 hr. This experiment started at the same time as that in Figures 2a–2c. The same map projection and height color coding as those in Figure 2 are applied. Note the particle number density used here is much less. (d) Surface wind stress (color), ~130 m winds (vector) and surface pressure perturbation (Pa, contour) when the low pressure of the storm shown in Figure 2b passes 0°E.

location of strong Hadley return flow during the daytime, i.e., the western boundary currents [*Wilson and Hamilton*, 1996]. They are also associated with strong storm tracks [*Hollingsworth et al.*, 1996]. The coincidence of strong frontal storm development and enhanced Hadley/tidal flow in these regions allows southward motion of fronts associated with low pressure storms. Lower-resolution GCM simulations show interannual variability in the strength of the Acidalia-Chryse eddies between pre- and post-solstice seasonal windows, and indicate variability of the timing of strong southward frontal motion within these windows. The likely number of storms with significant southward motion can be estimated as the following. The seasonal windows are continuously open for only ~50 sols (~30° of Ls). If we take the period of the baroclinic disturbances to be ~2 sols, then ~25 storms will pass through Acidalia in each seasonal window. The "tidal gate" is open for ~10 hours each day, or ~40% of the time. This suggests that ~10 storms will have the opportunity to flush particles to the low latitudes. Of these, some will not have a timely strong trailing high pressure, some will lie at too high of a latitude. The model suggests that this will happen about half of the time, generating ~5 events per window. This is in rough agreement with the MGS observations.

3. Discussion

[11] The largest dust storm in MGS mapping year 1 is associated with several southward moving dust fronts, occurring within days of each other in Acidalia-Chryse. The observations suggest that such fronts in rapid succession is responsible for the development of large dust storms. GCM simulations suggest that the determinants of whether fronts move southward are local time and season. Local time determines whether the frontal winds synchronously mesh with the tidal winds to generate southward transport. The season determines whether suitable fronts develop. As the seasonal windows are short, and the shortest period of the baroclinic waves is ~2 sols [*Wilson et al.*, 2002], there exist few cycles within a given seasonal window for baroclinic storms to synchronize with the tidal flow. Variability within these windows can therefore be generated by the random initial phase and particular synoptic meteorology of the storms. If fronts do not become well synchronized with the tidal flow, southward frontal motion will be diminished or even inhibited. On the other hand, if the phasing and meteorology are favorable, several successive dust fronts could be transported into the southern subtropics. *Haberle et al.* [1982] and *Wilson* [1997] demonstrated that injection of dust into the Hadley convergence zone enhances the Hadley circulation, spreading the dust deep into the atmosphere, increasing mid-level air temperatures, and producing global dust storm signatures. The stochastic aspect, resulting from frontal phasing and meteorology then provides a mechanism for interannual variability in this type of large dust storms. *Newman et al.* [2002] have shown that if surface winds are coupled to dust injection, global models can generate southward moving storms similar to those observed in Acidalia-Chryse, with year-to-year variability.

[12] This paper suggests a mechanism for large dust storm triggering. It provides an example of the interaction of major circulation systems on Mars. Nonetheless, important issues, such as radiative-dynamical feedbacks and a quantitative estimate of the amount of dust needed in the southern tropics for the development of "global impact," have not been addressed. In addition, we only explain the largest dust storm occurred in the first MGS mapping year, and the particular mechanism does not apply generally to all martian dust storms.

References

Barnes, J. R., J. B. Pollack, R. M. Haberle, C. B. Leovy, R. W. Zurek, H. Lee, and J. Schaeffer, Mars atmospheric dynamics as simulated by the NASA Ames general-circulation model: 2. Transient baroclinic eddies, *J. Geophys. Res.*, *98*(E2), 3125–3148, 1993.

Cantor, B. A., P. B. James, M. Caplinger, and M. J. Wolff, Martian dust storms: 1999 Mars Orbiter Camera observations, *J. Geophys. Res.*, *106*(E10), 23,653–23,687, 2001.

Eluszkiewicz, J., R. A. Plumb, and N. Nakamura, Dynamics of wintertime stratospheric transport in the Geophysical Fluid Dynamics Laboratory SKYHI general circulation model, *J. Geophys. Res.*, *100*(D10), 20,883–20,900, 1995.

Haberle, R. M., Interannual variability of global dust storms on Mars, *Science*, *234*(4775), 459–461, 1986.

Haberle, R. M., C. B. Leovy, and J. B. Pollack, Some effects of global dust storms on the atmospheric circulation of Mars, *Icarus*, *50*(2–3), 322–367, 1982.

Hinson, D. P., and R. J. Wilson, Transient eddies in the southern hemisphere of Mars, *Geophys. Res. Lett.*, *29*(7), 1154, doi:10.1029/2001GL014103, 2002.

Hollingsworth, J. L., R. M. Haberle, J. R. Barnes, A. F. C. Bridger, J. B. Pollack, H. Lee, and J. Schaeffer, Orographic control of storm zones on Mars, *Nature*, *380*, 413–416, 1996.

James, P. B., J. L. Hollingsworth, M. J. Wolff, and S. W. Lee, North polar dust storms in early spring on Mars, *Icarus*, *138*(1), 64–73, 1999.

Liu, J., M. I. Richardson, and R. J. Wilson, An assessment of the global, seasonal, and interannual spacecraft record of Martian climate in the thermal infrared, *J. Geophys. Res.*, *108*, doi:10.1029/2002JE001921, in press, 2003.

Newman, C. E., S. R. Lewis, P. L. Read, and F. Forget, Modeling the Martian dust cycle: 2. Multiannual radiatively active dust transport simulations, *J. Geophys. Res.*, *107*(E12), 5124, doi:10.1029/2002JE101920, 2002.

Pankine, A. A., and A. P. Ingersoll, Interannual variability of martian global dust storms-Simulations with a low order model of the general circulation, *Icarus*, *155*(2), 209–323, 2002.

Richardson, M. I., and R. J. Wilson, Investigation of the nature and stability of the Martian seasonal water cycle with a general circulation model, *J. Geophys. Res.*, *107*(E5), 5031, doi:10.1029/2001JE001536, 2002.

Smith, M. D., J. C. Pearl, B. J. Conrath, and P. R. Christensen, Thermal Emission Spectrometer results: Mars atmospheric thermal structure and aerosol distribution, *J. Geophys. Res.*, *106*(E10), 23,929–23,945, 2001.

Smith, M. D., R. J. Conrath, J. C. Pearl, and P. R. Christensen, Thermal Emission Spectrometer observations of Martian planet-encircling dust storm 2001A, *Icarus*, *157*(1), 259–263, 2002.

Wang, H., and A. P. Ingersoll, Martian clouds observed by Mars Global Surveyor Mars Orbiter Camera, *J. Geophys. Res.*, *107*(E10), 5078, doi:10.1029/2001JE001815, 2002.

Wilson, R. J., A general circulation model simulation of the Martian polar warming, *Geophys. Res. Lett.*, *24*(2), 123–126, 1997.

Wilson, R. J., and K. Hamilton, Comprehensive model simulation of thermal tides in the Martian atmosphere, *J. Atmos. Sci.*, *53*(9), 1290–1326, 1996.

Wilson, R. J., D. Banfield, B. J. Conrath, and M. D. Smith, Traveling waves in the Northern Hemisphere of Mars, *Geophys. Res. Lett.*, *29*(14), 1684, doi:10.1029/2002GL014866, 2002.

Zurek, R. W., et al., Dynamics of the atmosphere of Mars, in *Mars*, edited by H. H. Keiffer, B. M. Jakosky, C. W. Snyder, and M. S. Matthews, pp. 835–933, Univ. Arizona Press, Tucson, 1992.

A. P. Ingersoll, M. I. Richardson, and H. Wang, Division of Geological and Planetary Sciences, California Institute of Technology, MC 150-21, Pasadena, CA 91125, USA. (hqw@gps.caltech.edu)

A. D. Toigo, Center for Radiophysics and Space Research, Cornell University, Ithaca, NY 14853, USA.

R. J. Wilson, NOAA/Geophysical Fluid Dynamics Laboratory, Princeton, NJ, USA.

R. W. Zurek, Jet Propulsion Laboratory, California Institute of Technology, Pasadena, CA 91109, USA.